Experimental Study on the Organic Rankine Cycle for Recovering Waste Thermal Energy

Soo-Yong Cho*‡, Yang-Beom Jung**, Chong-Hyun Cho***

*Department of Aerospace & System Engineering (ReCAPT), Gyeong-Sang National University, 501 Jinju-daero, Gyeong-Nam, Jinju 52828, Republic of Korea

** R&D Center, BIP Ltd, Busan 46273, Republic of Korea

*** R&D Center, Suntech Ltd, Jen-Nam, Soon-Cheon 57949, Republic of Korea

(sycho@gnu.ac.kr, ybjung@bn-bip.com, air0427@empas.com)

‡ Corresponding Author; Soo-Yong Cho, Tel: +82 55 772 1586, Fax: +82 55 772 1580, sycho@gnu.ac.kr

Received: 29.05.2017 Accepted:25.07.2017

Abstract- The organic Rankine cycle (ORC) has been using to convert renewable energy, such as waste heat, solar energy, geothermal energy and so on, to mechanical energy or electrical energy. In general, these kinds of renewable energies cannot be constantly supplied, and so the ORC should operate at various working conditions. For example, waste energy at a factory is usually varied depending on the type of production process. Hence, the ORC must be operated at off-design points due to the fluctuation of the available thermal energy. Its performance at off-design points can be worse than expected, since the components used in the ORC system are matched to the design point. When the ORC system is operated at a far off-design point, its output does not reflect its actual performance. This study investigated the performance of an ORC operating at far off-design points with components that were appropriately matched to its operating condition. In order to investigate the effect of the components used in the ORC system, the experimental results were compared with the performance of the ORC that was designed with components matched to the design point. The compared results showed that the efficiency of the ORC system at far off-design points could be greatly improved when the components used in the ORC system were matched appropriately to the actual ORC operating condition.

Keywords Low Thermal Energy Recovery, Fluctuating Thermal Energy, Experiment, Organic Rankine Cycle, Performance Improvement.

1. Introduction

Concerns for climate change due to fossil fuel emissions and the depletion of fossil fuels have stimulated studies focused on developing renewable energy technologies and efforts to increase the proportion of renewable energy in the world's total energy consumption. These efforts have also contributed to the increasing utilization of renewable energy from various energy sources, including solar, geothermal, waste heat, ocean energy, biomass, wind energy and so on. Among renewable energy technologies, the organic Rankine cycle (ORC) has been used to produce mechanical energy or electricity from thermal energy. For thermal energy sources with large capacity and high temperature, the ORC is a superb energy conversion approach among many feasible methods. In the case of solar energy, the ORC has been used to generate electricity from a thermal energy source achieved by collecting the sun's light using reflecting mirrors. Even if an available thermal energy source does not have a high temperature, the ORC can still be a good energy convertor, because it can exploit wide differences in temperature [1-5]. For instance, the ORC has been applied to produce electricity using the temperature difference between the sea surface and deep sea, which is not possible for any typical power generator. This advantage also allow the ORC to be used to generate electricity from waste heat that is discarded in industries, incinerators, fuel cells and so on.

Unlike typical power generators which can produce electricity without any difficulty only if a heat source has enough capacity and a high temperature, the ORC can utilize a variety of heat sources. In the field of renewable energy, most studies have focused on developing new energy sources

or technologies which can utilize sources of energy that are not suitable for typical power generators. For example, this would include thermal energy from a heat source that had small capacity or low temperature. In addition, most thermal energy is not available continuously, i.e., thermal energy produced from the sun can vary depending on the geographical location or time [6, 7], and thermal energy from the waste heat exhausted by industries also varies depending on the type of process and operations. However, one of the advantages of the ORC is that the ORC can still produce output power even though the available thermal energy fluctuates.

Many different types of organic compounds can be used as the operating fluid of an ORC. Accordingly, a large number of studies have been conducted to determine the most efficient organic compounds to be used as the ORC operating fluid [8-15]. The most important characteristics of the operating fluid have been identified. First of all, the operating fluid of the ORC should have basic features, such as high efficiency, as well as non-toxic, low-cost, non-flammable, low global warming potential, and in particular, not be damaging to the ozone layer. To meet these requirements, natural refrigerants like carbon dioxide have sometimes been applied as the operating fluid of the ORC instead of other organic compounds [16]. However, carbon dioxide requires a system can work with high operating pressure at room temperature. In addition to that limitation, carbon dioxide has low critical temperature. As a result, most of operating fluids used for ORCs have been adopted from among refrigerants reformed from CFC/HFC refrigerants. However, a fairly wide number of refrigerants have been recommended for the operating fluid of particular ORC applications in the previous studies, since the operating performance of each refrigerant is dependent on the specific operating conditions of the ORC system being tested.

In previous ORC studies, many investigations have focused on improving the expander, because it is a core component in the conversion of thermal energy to mechanical energy. Depending on the available thermal energy capacity and its temperature, many different types of expanders have been adopted, including scroll, vane, screw, reciprocating, piston, turbo types, and so on [17-21]. While displacement type expanders have typically been used for small output power, turbo type expanders are usually applied for large output power. If the available thermal energy cannot be provided continuously, the operating set-point of the expander needs to be frequently changed. In such cases, the turbo expander is usually a better option because it can operate appropriately even at an off-design point.

In ORC applications, the choice of the expander as well as the operating fluid are critical. However, this choice ultimately depends on the available thermal energy capacity and its temperature. Hence, a cycle analysis for the ORC system should begin by correctly predicting the available thermal energy capacity and its temperature, and then a detailed design of the system can proceed.

Since the performance of the ORC is evaluated based on the output power produced by the generator, the efficiency of the ORC is affected by the performance of the components that make up the ORC system. As a result, the proper selection of components and the accurate design of parts used in the components are also key to the efficiency of the ORC. If the ORC operates at an off-design point far from the optimum design point due to fluctuations in the available thermal energy capacity, the ORC will not exhibit its true performance potential, because the components were designed to operate optimally for a different design point.

In this study, in order to investigate not only variations in the efficiency of the ORC by adopted components but also the true performance at a far off-design point, experiments were conducted on an ORC system (A-model) that was designed on the basis of the operating condition at a far off-design point. The experimental results were compared with the performance of the ORC system (B-model) that adopted the components designed at on-design point. The same facility was employed to remove any difference in losses on the experimental facility. From the comparison of two experimental results, the effect of components was investigated in the ORC system when the ORC should be operated at low output power due to the fluctuation of the available thermal energy source.

2. Experimental Facility

2.1. Composition of the ORC System

An ORC system was designed with an output power of 30kW to reflect the available thermal energy capacity for the purpose of utilizing the waste heat exhausted by a small or medium industry complex. A turbo-expander was adopted for the ORC because the waste heat available from industrial processes was not continuous or stable. To accommodate the situation where the waste heat was not provided continuously, a turbo-expander was designed to be operated in partial admission by adjusting the spouting area of the operating fluid to the expander, since operating in this condition is known to be more profitable than shutting-down when the available thermal energy is temporarily reduced.

When selecting the operating fluid, a few adoptable refrigerants were chosen from the many candidate refrigerants suggested in previous studies [8-15]. In particular, consideration was given to ensure that the operating fluid would be suitable for a system working with low thermal energy capacity. Since the temperature of the heat source was low, the evaporation and condensation temperature of the operating fluid needed to be precisely considered to properly compose a cycle. Based on these criteria, R134a, R245fa, R236ea, R245a and so on were chosen as adoptable refrigerants. Among them, R245fa was selected as the operating fluid after a cycle analysis determined it had the best efficiency [22].

Figure 1 shows the experimental facility that was used to measure the performance of the ORC with a turbo-expander operating at off-design point. It consists of an evaporator, regenerator, cooler, expander, generator, pump, tank and so on. Figure 2 shows the pressure-enthalpy (P-h) curve for the ORC cycle with the location of each component. During the process from 6a to 1 shown in Fig. 2, the operating fluid was

heated on the evaporator using Shell S2 thermal mass oil, and was changed from liquid to vapor. Then, after expanding through the nozzle in a state of the high pressure and temperature, it was used to rotate the rotor in the process from 1 to 3. This rotating power was converted to electricity by the generator. A recuperator was used to absorb the remaining thermal energy after operating the expander in the process from 3 to 3a. This thermal energy was used to warm the operating fluid which was supplied from the pump in the process from 6 to 6a. A cooler was used to change the vapor to liquid and this liquid was collected in the tank in the process from 3a to 5. The operating fluid in the tank was pressurized by the pump in the process from 5 to 6. Then the operating fluid flowed toward the recuperator in the process from 6 to 6a. Altogether, these processes constitute one cycle of the ORC.

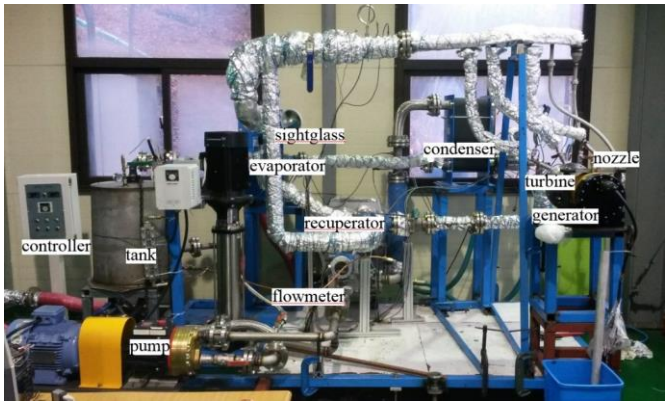

Fig. 1. Picture of the experimental facility for the regenerative organic Rankine cycle

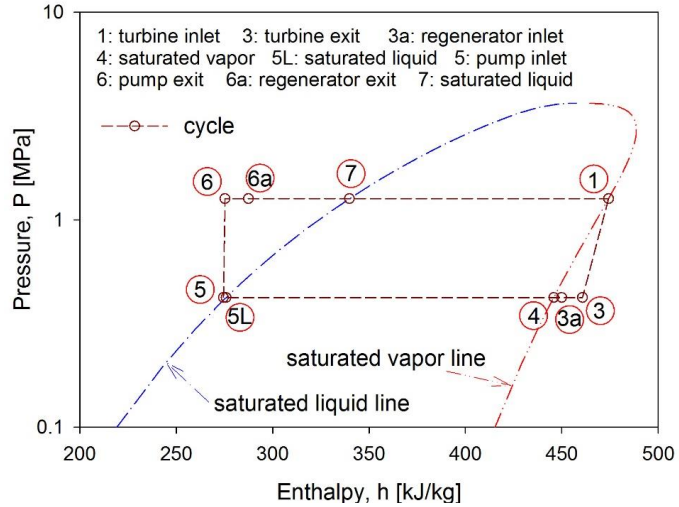

Fig. 2. Cycle of the ORC on the P-h curve with measuring locations

2.2. Instruments

In order to measure the temperature and pressure at the inlet and exit of each component, nine thermocouple and pressure sensors were installed. A mass flow meter was installed between the pump and the recuperator. The power-meter was used to measure the output power and the rotational speed of the generator. All data were saved in a PC using a data logger. Table 1 shows the model and accuracy of the instruments at full scale.

Table 1. Measuring instruments used in the experiment

Instrument	Maker	Model	Accuracy
Mass flowmeter	Endress+Hauser	80E15, Coriolis	$\pm$ 0.2%
Pressure sensor	Druck	PTX 7500	$\pm$ 0.05%
Thermometer	Dongyang	PT100	$\pm$ 0.2%
Power-meter	Yokogawa	WT1600	$\pm$ 0.1%
DAQ	Omron	ZR-RX45	$\pm$ 0.1%

2.3. Design of a Turbo-Expander

To operate the expander in partial admission, the rotor of the expander should be an impulse type design. With an impulse type rotor, not only should the blade profile be designed precisely according to the velocity triangle but the velocity of the operating fluid should also be determined, to ensure it is suitable for the expansion ratio. In the design of the impulse type turbo-expander, the rotor was chosen to a radial and cantilever type, as shown in Figure 3. The expander was designed to produce an output power of 29.6kW when operated at 21,000 RPM with a partial admission rate of 49.2% and a turbine inlet temperature of 110°C. The partial admission rate is defined as the ratio of the area at the nozzle exit to the area at the rotor inlet. The performance of the expander on the design point was predicted, and the design of the rotor was conducted using the results of the cycle analysis [23].

Fig. 3. Picture of turbine rotor connected to the generator rotor

For complete expansion in the impulse type expander, nozzles were adopted instead of a stator. The nozzle was designed simultaneously with the rotor in order to match the two parts. The rotor required the nozzle exit velocity to be Mach number 1.6 since the sonic speed of R245fa in a saturated state is approximately one third of the speed of sound. Hence, a convergent-divergent configuration of a circular cross-section was adopted. The spouting velocity at

the nozzle exit was obtained based on not only the nozzle shape but also operating conditions at the nozzle.

Based on the given temperature and pressure at the nozzle inlet, the convergent region toward the throat was designed using a nozzle design technique [23] based on the flow properties of R245fa. These flow properties were provided to the design program by interconnecting with Refprop [24]. The flow properties at the throat were used to design the divergent region, which was iteratively modified till the required velocity was obtained at the nozzle exit. In this process, the method of characteristics [25, 26] was applied because the state of the R245fa remained in the vapor state during the expansion. The pressure gradient [26] along the flow direction within the nozzle is derived from the continuity equation, momentum equation including the pressure drop that results from the change in the cross-sectional area, sonic speed, conservation of energy, and Gibbs equation as follows:

$$\frac{dP}{dx} = (1-M^2)^{-1}\left[\frac{\rho V^2}{A}\frac{dA}{dx} - \{(\rho V)^2\left(\frac{\partial \upsilon}{\partial s}\right)_p + \rho T\}\frac{V^2}{2T}\frac{f}{D}\right] \quad (1)$$

where M is Mach number, V is velocity, A is the cross-sectional area of the nozzle, s is entropy, ρ is density, T is temperature, f is friction coefficient, u is specific volume, D is diameter, and x is flow directional length. If the flow is chocked in the supersonic nozzle, the mass flowrate cannot be increased even though the pressure at the nozzle exit is lowered. Thus, the mass flowrate at the nozzle can be calculated at the nozzle throat when the flow is chocked. The designed nozzle shape was finally modified by considering the turbulent boundary layer thickness [27]. Figure 4 shows the nozzle shape and the contours of the Mach number within the nozzle.

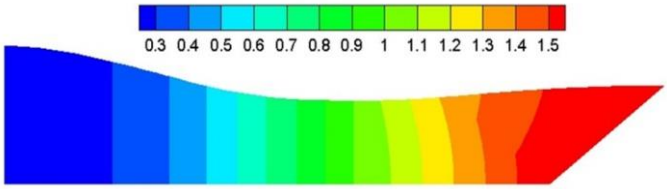

Fig. 4. Mach number contours and nozzle shape designed by the method of characteristics

2.4. Design of components

Figure 5 shows the cross-sectional view of the turbo-expander including a rotor, generator, bearings and so on. If the expander operates at a low turbine inlet temperature and a low partial admission rate due to the reduced thermal energy, the system efficiency could be low and this efficiency could not reflect its actual efficiency. This could happen if some of its components are not matched to the operating state at a far off-design point. For instance, if a generator, which was designed with an output power of 30kW, is actually operated at a far off-design point with an output power of less than 2 kW, the efficiency of the ORC includes the losses occurred on the large capacity generator. The core diameter of a large capacity generator is generally large. As a consequence, its rotational inertial force is also increased, and its cogging torque is increased as well. These factors could cause an increase of the losses on the generator if it is operated at low input power. Figure 6 shows the generator used in the experiment for low input power. This generator was designed on the basis of the output power of 5kW.

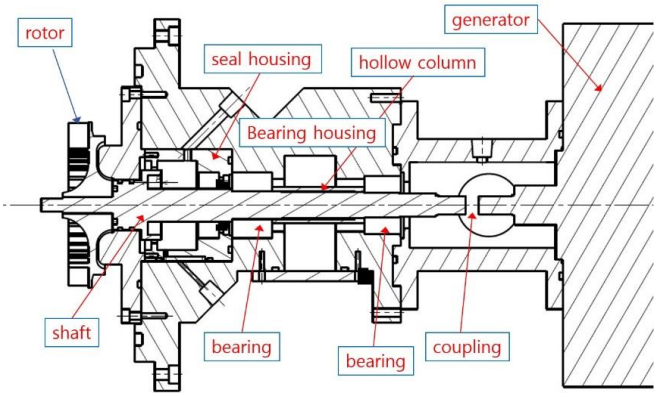

Fig. 5. Cross-sectional view of the turbo-expander

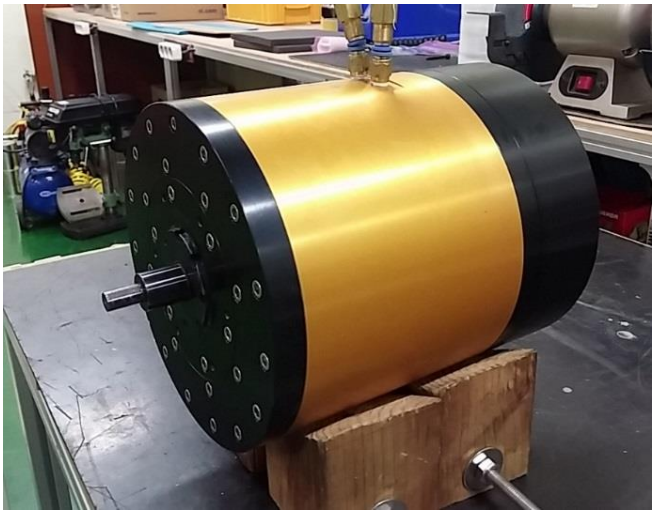

Fig. 6. 5kW generator fabricated for the experiment at off-design points

A bearing housing was fabricated as shown in Fig. 5, since the generator was not large enough to allow the rotor to be directly installed on the shaft of the generator. The rotor of the expander was installed on a shaft installed in the bearing housing, and this shaft was supported using two angular contact ball bearings. The gap between the two bearings was precisely adjusted using a hollow column so as not to transfer any axial load to the bearings during assembly of the parts. The shaft mounting the rotor was connected with the shaft of the generator using a flexible coupling.

The adoption of the bearing housing required another additional part to seal the operating fluid in the expander. For sealing the operating fluid, a seal housing was made for installation in the bearing housing. Figure 7 shows the seal housing and seals. Two kinds of seals were applied; a mechanical seal and a lip seal. Losses from the seal could greatly affect to the output power of the ORC. In the case of the mechanical seal, the two seal faces were kept in contact by a spring force. On a machine producing low output power

while working in a state of high pressure difference, the losses of the seal could be significantly increased due to the strong spring force. In the ORC, if the turbine inlet temperature decreased, the pressure difference between seal faces could be decreased. However, the spring force on the seal face could not be adjusted to match the temperature of the operating fluid while the ORC was working. For this reason, the lip seal instead of the mechanical seal was adopted to prevent losses. The lip seal was also in contact with the shaft. However, its losses were less than those of the mechanical seal. This reduction was possible due to the small shaft diameter, since the losses of the lip seal are affected by the shaft diameter. The shaft diameter was designed to be 20 mm. The adoption of the lip seal reduced the initial rotational torque by 50% compared with the mechanical seal.

Fig. 7. Seal housing, mechanical seal and lip seal

The electricity generated on the expander was dissipated on a load bank in the experiment. In addition, the output power on the expander was controlled by adjusting the resistances in the load bank. To obtain various resistance levels in response to variable loads, several resistances in the load bank were adjusted separately or in combination. If the variation of the output power is large, the adjusting step of the output power on the load bank could be large. If the expander is operated at a far off-design point, such as an output power of maximum 2 kW, the experiment should be performed with the more precisely adjusting step with various small capacity resistances. Hence, a load bank was fabricated based on the actual output power produced at the far off-design point. As a result, since the load bank can finely control the load with various resistances, the output power of the expander could be obtained at the optimal operating point.

In order to pressurize the operating fluid, many kinds of pumps can be applied. In the experiment using a turbo-type centrifugal pump, the mass flowrate of the operating fluid from the centrifugal pump was widely varied depending on the evaporating temperature. To constantly supply the mass flowrate from the centrifugal pump, a bypass valve was adopted since this method was better than adjusting the rotational speed of the pump. When the ORC system was being operated in a stable state, the turbo-type pump provided an advantage by constantly delivering the mass flow rate to the expander. However, the ORC system was sensitive when it operated at the off-design point. Therefore, in the experiment at the off-design points, a positive displacement type pump was adopted. The mass flow rate was controlled by varying the rotational speed of the pump. Due to the adoption of the positive displacement type pump, the mass flow rate pulsated a little. Nonetheless, the system was insensitive to operation at the off-design point.

3. Results and Discussion

The experiment was conducted using the same experimental facility to remove any discrepancies between on the A-model designed at off-design point and on the B-mode designed at on-design point. Hence, there was no different thermal losses occurring in different experimental facilities. In the experiment at off-design point, the mass flow rate supplied to the expander was controlled by the number of nozzles used. Maximum three nozzles were used among nine nozzles. The performance of the ORC was measured with various turbine inlet temperatures (T_{t1}). In the experiment, the number of nozzles on the expander was fixed, and the turbine inlet temperature was adjusted by controlling the thermal energy absorbed on the evaporator as well as the mass flow rate supplied from the pump. When the system was sufficiently stable, the measurement was performed. This stable operation was the state in which the thermal energy being absorbed by the operating fluid was equivalent to the thermal energy supplied from the heat source. In this state, the operation of the ORC became self-sustaining.

$$\eta_{sys} = \frac{W_{out} - W_{pump}}{\dot{m}(h_{t1} - h_{t6a})} \tag{2}$$

The system efficiency of the ORC was evaluated as in Eq. (2). The numerator in Eq. (2) was the actual output power that was obtained from the output power on the generator (W_{out}) after removing the power consumed by the pump (W_{pump}). The power consumed by the pump was estimated to be $\dot{m}(h_{t6} - h_{t5})$ where h_{t5} and h_{t6} mean the total enthalpy at the inlet and exit of the pump, respectively. The locations used to measure the total enthalpy marked with numbers in Figure 2. The thermal energy absorbed by the evaporation was used as the input power for the system efficiency. It was obtained from the total enthalpy at the inlet of the evaporator (h_{t6a}) and at the inlet of the expander (h_{t1}). Hence, the system efficiency could be increased if the input power for the system was reduced or the output power increased. The input power can be reduced if the system uses more efficient components or the losses on the system are reduced. In this experiment, the efficiency of the system was measured after improving the parts linked to the expander based on the actual output power.

Even if various thermal energies have been used to the ORC, the available thermal energy could have large capacity with low temperature or small capacity with high temperature. Depending on the condition of the available thermal energy, the number of nozzles on the expander was controlled based on the turbine inlet temperature. The experiment was conducted by varying the turbine inlet

temperature as well as the number of nozzles used. Although measurements were conducted when the system was operating in a stable state, the measured results could be different depending on the state of the operating fluid at the inlet of the expander. The state of the fluid was determined by the mass flow rate and the supplied thermal energy, and consequently it could be wet, saturated, or superheated. Measurements were performed when the operating fluid at the inlet of the expander was maintained in a state of saturated vapor.

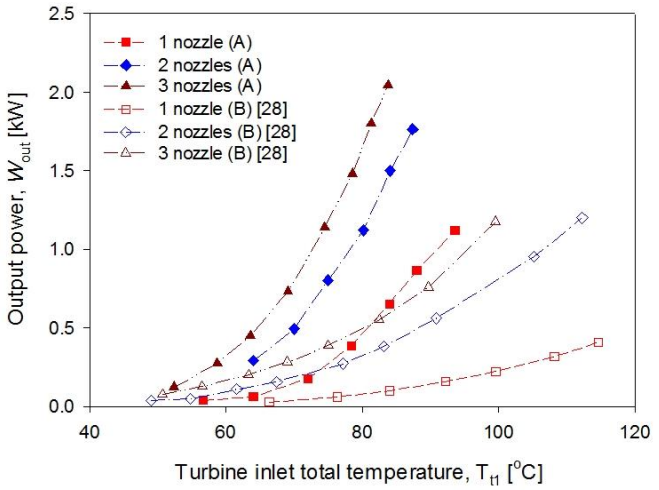

Fig. 8. Comparison of the output power versus turbine inlet temperature

Figure 8 shows the variation of the output power produced by the generator with various turbine inlet temperatures and according to the number of nozzles used. Not only was the output power on the A-model increased, but its growth rate was also increased by changes in the turbine inlet temperature. This increase in output power resulted from the parts that were designed to match its actual output power. The increase in output power could mean that the performance of the ORC was improved if the mass flow rate was same. Thus, the mass flow rate was checked, as shown in Fig. 9. The mass flow rate was nearly equivalent to that of the B-model [28] when the ORC was operated under the same conditions. Hence, this result meant that the performance of the A-model was improved.

The variation in the output power showed trends quite similar to the variation in the turbine inlet temperature. The output power was naturally increased with increases in the mass flow rate, or the turbine inlet temperature, but it did not increase linearly. Its growth rate was increased when the turbine inlet temperature was increased with a large mass flow rate. In the results of the output power, a small amount of output power was obtained when the turbine inlet temperature was decreased, even to 50°C. It would be possible to increase this output power by increasing the mass flow rate, if the system was operating with a large thermal energy capacity. If the expander is operated with an increased mass flow rate, the efficiency of the expander is also improved because the partial admission rate is increased. In this experiment, the partial admission rate was 5.4 % when one nozzle was applied.

Figure 9 shows the variation in the mass flow rate according to the turbine inlet temperature. The difference between the two experiments was insignificant. This is a natural outcome because the flow at the exit of the nozzle was supersonic. A slight difference between the two experiments could be caused by a difference in the density of the operating fluid at a superheated temperature. The mass flow rate in the supersonic nozzle is changed if the temperature is changed even though it is choked at the throat. The experimental result also showed that the mass flow rate was increased when the turbine inlet temperature increased, since the increase in the turbine inlet temperature was accompanied by an increase in the density due to the increased pressure.

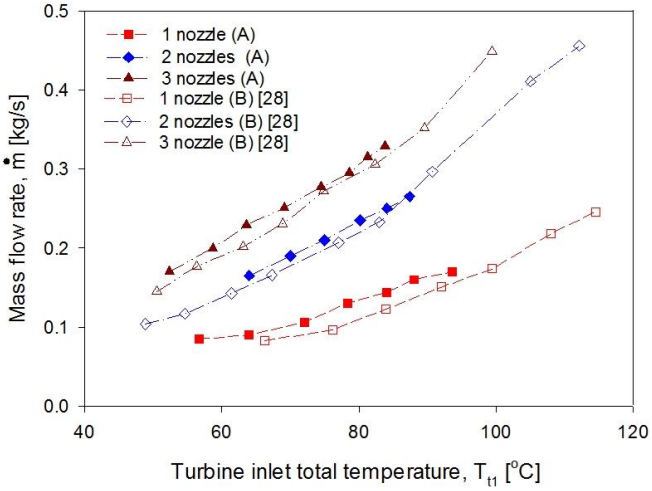

Fig. 9. Variation of the mass flow rate for the various turbine inlet temperatures

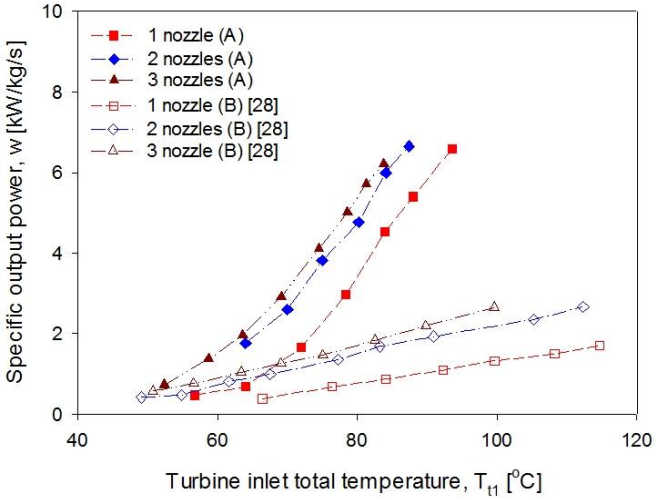

Fig. 10. Comparison of the specific output power versus turbine inlet temperature

Figure 10 shows the variation in the specific output power (w) obtained from the output power with the mass flow rate. Since the specific output power on the A-model was increased, its performance was greatly improved. However, the two experimental results showed similar trends, for example, the growth rate of the specific output power was decreased when the number of nozzles used was increased from two to three, as compared with when it was

increased from one to two. The reason for this is that the output power was not proportionally increased for the number of nozzles used even though the mass flow rate was increased proportionally. In actuality, the output power can increase proportionally for the mass flow rate if the efficiency of the expander is kept constant. However, in partial admission, the efficiency of the expander increased with the increase in the partial admission rate. The growth rate in the efficiency of the expander was maximized in the low partial admission rate. For this reason, the growth rate of the specific output power was also increased in the low partial admission rate.

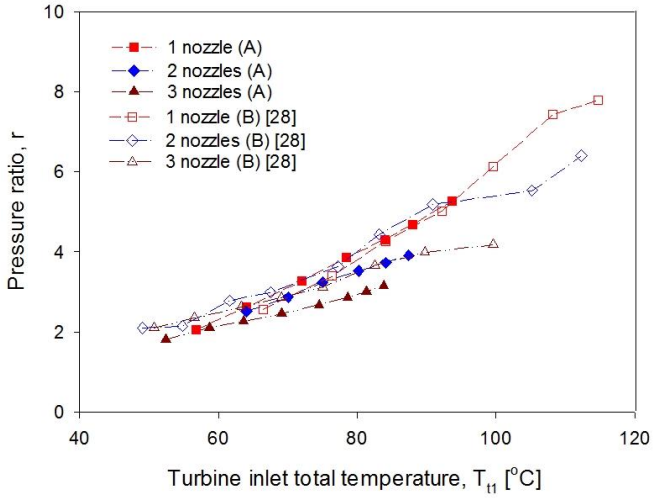

Fig. 11. Variation of the expansion ratio versus turbine inlet temperature

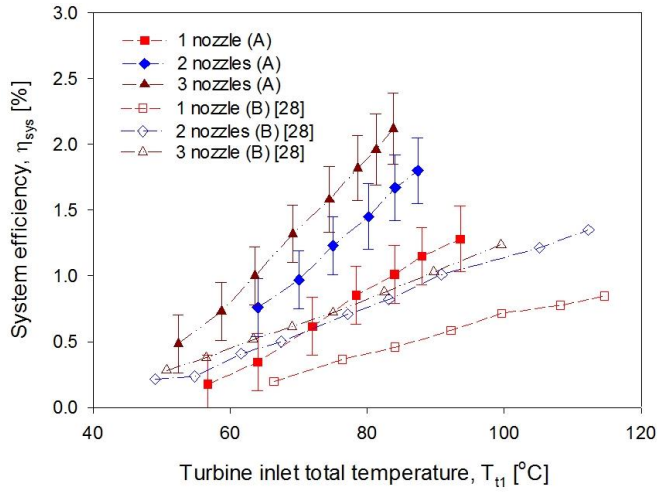

Fig. 12. Comparison of the system efficiency with uncertainty band

Figure 11 shows the expansion ratio ($r = P_{t1} / P_{t3}$) obtained using the total pressure at the inlet and exit of the expander. The two experimental results illustrated similar trends for the variation in the turbine inlet temperature. The expansion ratio greatly depended on the pressure at the exit of the expander. This pressure was determined by the temperature of the cooler. This temperature was precisely controlled by a large refrigerator for the two experiments so that the temperature of the cooler was kept constant. For this reason, the two results were quite similar, even though the result of the A-model was slightly lower than that of the B-model. The lower expansion ratio of the A-model seems to have occurred because the experiment was conducted with the turbine inlet temperature close to saturated vapor.

Figure 12 shows the variation in the system efficiency for the number of nozzles used, and the turbine inlet temperature. As shown in the results of the specific output power, the system efficiency was increased by the experiment in the A-model. However, even though the system efficiency was increased in the A-model, it still seems too low for application in the field. This could be because the expander was operated in a low partial admission rate as well as with a low turbine inlet temperature. If this system was operated with an increased partial admission rate and with a high temperature heat source, its system efficiency could be greater than 10 %. Like the growth rate of the specific output power, the growth rate of the system efficiency was also alleviated when the number of nozzles used was increased.

An uncertainty analysis of the system efficiency was conducted [29, 30] using the system efficiency formulated in Eq. (2) with the six measured variables (x_i) which were the output power, mass flow rate, and the four enthalpies of h_{t1}, h_{t5} , h_{t5} , h_{t6a} . The uncertainty ($U_{\eta_{sys}}$) of the system efficiency was obtained using Eq. (3) with the uncertainty of measured variables (U_{x_i}). As shown in Figure 12, each uncertainty band is illustrated with the measured data.

$$\frac{U_{\eta_{sys}}}{\eta_{sys}} = \pm[\sum_{i=1}^{6} (\frac{x_i}{\eta_{sys}} \frac{\partial \eta_{sys}}{\partial x_i})^2 (\frac{U_{x_i}}{x_i})^2]^{1/2} \quad (3)$$

4. Conclusion

This experiment was conducted to investigate the effect of the components composing the ORC system. The components including the generator, seal, bearing, load bank and so on were designed to be compatible with the actual operating conditions of the ORC at a far off-design point. The experimental results were compared with the experimental results that were obtained in the ORC system composing with the components designed at on-design point. In the experiment with the ORC system designed at on-design point, its performance at the far off-design point could not reflect its actual performance if the losses occurred in the components were not considered. When the ORC system was operated with the component designed at its actual output power, the specific output power and the system efficiency were improved, such that the system efficiency was increased from 0.82% to 1.85% for the turbine inlet temperature of 80°C with three nozzles. Thus, this result demonstrates that the performance of the ORC system can be greatly affected by its components when it is operated at a far off-design point.

Acknowledgements

This research was financially supported by the Korea institute of Energy Technology Evaluation and Planning (KETEP) funded by the Ministry of Trade, Industry & Energy (MOTIE) of Korea Government.

References

[1] H.D.M. Hettiarachchi, M. Golubovic, W.M. Worek, and Y. Ikegami, "Optimum design criteria for an organic Rankine cycle using low-temperature geothermal heat sources", Energy, 2007, Vol. 32, pp. 1698-1706.

[2] G. Qiu, Y. Shao, J. Li, H. Liu, and S. Riffat, "Experimental investigation of a biomass-fired ORC-based micro-CHP for domestic applications", Fuel, 2012, Vol. 96, pp. 374-382.

[3] J. Navarro-Esbrí, B. Peris, R. Collado, and F. Molés, "Micro-generation and micro combined heat and power generation using free low temperature heat sources through organic Rankine cycles", In International conference on renewable energies and power quality (ICREPQ'13), Bilbao, Spain, 20-22 March 2013. (Conference Paper)

[4] B. Twomey, P.A. Jacobs, and H. Gurgenci, "Dynamic performance estimation of small scale solar cogeneration with an organic Rankine cycle using a scroll expander", Applied Thermal Engineering. 2013, Vol. 51, pp. 1307-1316.

[5] A.R. Noorpoor, and S. Heidararab, "Exergoeconomic Assessment, Parametric Study and Optimization of a Novel Solar Trigeneration System", International Journal of Renewable Energy Research, 2016, Vol. 6, No. 3, pp. 795-816.

[6] A. Bensenouct, and A. Medjelled, "Thermodynamic and efficiency analysis of solar steam power plant cycle", International Journal of Renewable Energy Research, 2016, Vol. 6, No. 4, pp. 1556-1564.

[7] G.J.J. Wessley, R.N. Starbell, and S. Sandhya, "Modelling of Optimal Tilt Angle for Solar Collectors Across Eight Indian Cities", International Journal of Renewable Energy Research, 2017, Vol. 7, No. 1, pp. 353-358.

[8] V. Maizza, and A. Maizza, "Working fluids in non-steady flows for waste energy recovery systems. Applied Thermal Engineering", 1996, Vol. 16, pp. 579-590.

[9] T.C. Hung, T.Y. Shai, and S.K. Wang, "A review of organic Rankine cycles for the recovery of low-grade waste heat", Energy, 1997, Vol. 22, pp. 661-667.

[10] B.T. Liu, K.H. Chie, and C.H. Wang, "Effect of working fluids on organic Rankine cycle for waste heat recovery", Energy, 2004, Vol. 29, pp. 1207-1217.

[11] B.F. Tchanche, G. Papadakis, G. Lambrinos, and A. Frangoudakis, "Fluid selection for a low-temperature solar organic Rankine cycle", Applied Thermal Engineering, 2009, Vol. 29, pp. 2468-2476.

[12] T.C. Hung, S.K. Wang, C.H, Kuo, B.S. Pei, and K.F. Tsai, "A study of organic working fluids on system efficiency of an ORC using low-grade energy sources", Energy, 2010, Vol. 35, pp. 1403-1411.

[13] H. Chen, D.Y. Goswami, and E.K. Stefanakos, "A review of thermodynamic cycles and working fluids for the conversion of low-grade heat", Renewable Sustain Energy Rev., 2010, Vol. 14, pp. 3059-3067.

[14] F. Velez, J.J. Segovia, M.C. Martín, G. Antolín, F. Chejne, and A. Quijano, "A technical, economical and market review of organic Rankine cycles for the conversion of low-grade heat for power generation", Renewable Sustain Energy Rev., 2012, Vol. 16, pp. 4175-4189.

[15] J. Bao, and L. Zhao, "A review of working fluid and expander selections for organic Rankine cycle", Renewable Sustain Energy Rev., 2013, Vol. 24, pp. 325-342.

[16] B. Yang, X. Peng, Z. Hea, B. Guo, and Z. Xing, "Experimental investigation on the internal working process of a CO2 rotary vane expander", Applied Thermal Engineering, 2009, Vol. 29, pp. 2289-2296.

[17] S. Quoilin, V. Lemort, and J. Lebrun, "Experimental study and modeling of an organic Rankine cycle using scroll expander", Applied Energy, 2010, Vol. 87, pp. 1260-1268.

[18] W. Wang, Y. Wu, C. Ma, L. Liu, and J. Yu, "Preliminary experimental study of single screw expander prototype", Applied Thermal Engineering, 2011, Vol. 31, pp. 3684-3688.

[19] B. Zhang, X. Peng, Z. He, Z. Xing, and P. Shu, "Development of a double acting free piston expander for power recovery in transcritical CO2 cycle", Applied Thermal Engineering, 2007, Vol. 27, pp. 1629-1636.

[20] G Qiu, H. Liu, and S. Riffat, "Expanders for micro-CHP systems with organic Rankine cycle", Applied Thermal Engineering, 2011, Vol. 31, pp. 3301-3307.

[21] T. Yamamoto, T. Furuhata, N. Arai, and K. Mori, "Design and testing of the organic Rankine cycle", Energy, 2001, Vol. 26, pp. 239-251.

[22] S.Y. Cho, and C.H. Cho, "Selection of working fluid on the organic Rankine cycle to utilize low-temperature waste heat", J. Korean Soc New & Renew Energy, 2014, Vol. 10, pp. 36-46.

[23] S.Y. Cho, C.H. Cho, K.Y. Ahn, and Y.D. Lee, "A study of the optimal operating conditions in the organic Rankine cycle using a turbo-expander for fluctuations of the available thermal energy", Energy, 2014, Vol. 64, pp. 900-911.

[24] NIST. "Reference fluid thermodynamics and transport properties", Refprop Version 9.0, 2009.

[25] M.J. Zucrow, and J.D. Hoffman, Gas dynamics, John Wiley & Sons Inc., 1976,Vol. 2, pp.185-265. (Book)

[26] B.K. Hodge, and K. Koenig, Compressible fluid dynamics with personal computer application, Prentice Hall, New Jersey, 1995, pp. 435-487. (Book)

[27] P.S. Granville, "The determination of the local skin friction and the thickness of turbulent boundary layers from the velocity similarity laws", David W. Taylor model basin report 1340. 1959.

[28] S.Y. Cho, and C.H. Cho, "An experimental study on the organic Rankine cycle to determine as to how efficiently utilize fluctuating thermal energy", Renewable Energy, 2015, Vol. 80, pp. 73-79.

[29] S.Y. Cho, and C. Park, "A study on the propagation of measurement uncertainties into the result on a turbine performance test", KSME inter. J. 2004, Vol. 18, pp. 689-698.

[30] H.W. Coleman, and W.G. Steels, Experimentation and uncertainty analysis for engineers, John Wiley & Sons Inc., 1999, pp. 83-129. (Book)